International Journal of Thermophysics, Vol. 17, No. 5, 1996

Thermophysical Properties of Tungsten Electrodes by Subsecond Pulse Calorimetry[1]

N. Lj. Perović,[2,3] K. D. Maglić,[2] and G. S. Vuković[2]

Prediction of the behavior of tungsten electrode material in high-temperature plasma generators requires knowledge of its thermophysical properties over a wide temperature range. For determination of its relevant thermophysical properties, the direct pulse heating calorimetry technique was chosen as the most appropriate, as it meets requirements of both high-speed measurements and the widest temperature range. As a high-temperature sensor, the method used simultaneously a fine-gauge thermocouple and an optical pyrometer. Such a combination enables coverage of a few thousand degrees within a second, with a time resolution of less than 1 ms. The measurement technique and details of the apparatus as well as experimental results for specific heat, electrical resistivity, normal spectral, and hemispherical total emittance in the temperature range from 300 to 2500 K are presented.

KEY WORDS: electrical resistivity, hemispherical total emittance; normal spectral emittance, pulse heating; specific heat; subsecond calorimetry; tungsten.

1. INTRODUCTION

The present study on tungsten electrode is a part of a study of thermal and electrical properties of refractory metals at the Thermophysical Properties Laboratory of the Institute of Nuclear Sciences VINČA. The data are important for prediction of the behavior of this material in high-temperature plasma generators. In addition to providing data on specific heat and electrical resistivity of the investigated metal, research described in this paper has increased the upper temperature limit of the measurements

[1] Paper presented at the Fourth International Workshop on Subsecond Thermophysics, June 27–29, 1995, Köln, Germany.

[2] Institute of Nuclear Sciences Vinča, P.O. Box 522, 11001 Belgrade, Serbia.

[3] To whom correspondence should be addressed.

0195-928X/96/0900-1047$09.50/0

to 2500 K and has, in the range above 1000 K, enabled generation of data on both hemispherical total emittance and normal spectral emittance. As the subsecond pulse calorimetry based on pyrometric temperature measurements [1–3] provides good and reliable data above 1500 K, this variant of the subsecond pulse calorimetry using contact thermometry from 300 to 2500 K has also provided an overlap between the two calorimetric techniques. In contrast to the previously used combination of base metal and noble metal thermocouples, which limited its application to 1900 K, in this study the temperature limit was increased to 2500 K by employing a tungsten–5% rhenium/tungsten–26% rhenium thermocouple. Simultaneous measurements in the temperature range where thermocouples and optical pyrometer overlap provided information which allowed computation of normal spectral emittance of the specimen.

2. MEASUREMENTS

2.1. Specimen

The tungsten electrode specimen was originally manufactured in the shape of a rod 2.4 mm in diameter and 175.2 mm in length and was directly used in the measurements. The specimen was not thermally treated prior to pulse experiments. The chemical analysis of the specimen is given in Table I.

2.2. Procedure

The specific heat, hemispherical total emittance, normal spectral emittance, and electrical resistivity of the tungsten electrode specimen were

Table I. Chemical Analysis of the Tungsten Electrode Specimen ($mg \cdot kg^{-1}$)

Al	Ba	Be	Ca	Cd	Co	Cr	Cu
512	<10	<10	<10	<10	<10	<10	<10
Fe	Ga	Mg	Mn	Mo	Ni	P	Pb
<10	<10	<10	<10	<10	<10	<10	<10
Si	Sn	Sr	Ti	Th	Va	Zn	Zr
<10	<10	<10	<10	<5	<10	<10	<10

measured simultaneously by a pulse heating method described in Ref. 4, which involved fast resistive heating of the specimen from room temperature to a predetermined maximum temperature, with simultaneous measurement of the temperature, voltage drop, and current through the specimen. Direct current pulses of 150–1500 A, from one or two heavy-duty 12-V batteries connected in series, enabled the specimen to heat at rates up to 4000 $K \cdot s^{-1}$.

One Tungsten–5% Rhenium/Tungsten–26% Rhenium thermocouple, 0.1 mm in diameter, was welded intrinsically in the middle of the specimen for measurement of its temperature. At the ends of specimen measurement zone, at a 30-mm separation, two 0.1-mm tungsten wire potential leads were welded for the voltage drop measurement. All measurements were performed in vacuum (10^{-3} Pa).

The experiments were performed under the control of a PC, which was used for real-time data acquisition and their subsequent processing. Data on current, voltage drop across the measurement zone, thermocouple emf, and pyrometer output were recorded at a sampling frequency of 1 to 10 kHz, during specimen heating lasting up to 750 ms, and during the initial part of the cooling period. Several thousand data points were recorded per experiment yielding 500–1000 values of specific heat, electrical resistivity, hemispherical total emittance, and normal spectral emittance in the temperature range studied.

In the experiments where pyrometric measurements were performed, a monochromatic optical pyrometer operating at 0.9 μm was sighted at the center of the specimen, close to the position of the central thermocouple. The pyrometer spot covered the circular target 0.75 mm in diameter at the specimen surface.

The specific heat capacity was computed from

$$C_p = \frac{(UI - P_r)}{m(dT/dt)_h} \tag{1}$$

and the electrical resistivity

$$\rho = \frac{U}{I}\frac{S}{L_e} \tag{2}$$

where U is the voltage drop across the effective specimen length between the potential leads, L_e; I is the current; P_r is the radiative power loss from the measurement zone; m is the mass of the effective specimen; $(dT/dt)_h$ is the heating rate at a given temperature; and S is the specimen cross section.

The radiative power loss, P_r, in Eq. (1) is expressed by

$$P_r = \varepsilon_{ht} \sigma A (T^4 - T_0^4) \tag{3}$$

where T_0 and T are the absolute temperatures of the ambient and the specimen, respectively, A is the specimen surface area, σ is the Stefan–Boltzmann constant, and ε_{ht} is the hemispherical total emittance. The latter is computed at different temperatures from experimental data obtained during both the heating and the cooling periods of experiments ending at these temperatures, using the expression

$$\varepsilon_{ht} = \frac{UI}{\sigma A (T^4 - T_a^4)[1 - (dT/dt)_h/(dT/dt)_c]} \tag{4}$$

Data collected during the experiments with simultaneous pyrometric measurements enabled determination of normal spectral emittance. The latter was computed using

$$\varepsilon_{ns} = \exp\left[\frac{c_2}{\lambda}\left(\frac{1}{T} - \frac{1}{T_b}\right)\right] \tag{5}$$

where T is the true temperate e of the specimen measured with the thermocouple, T_b is the brightness temperature of the specimen measured with the optical pyrometer, λ is the pyrometer effective wavelength, and c_2 is the second radiation constant.

3. RESULTS

A total of 15 experiments was performed, in which experimental conditions, such as heating rate, maximum temperature attained, current direction, and sampling frequency, were varied. Pyrometric measurements were performed in ten experiments. For the final processing, seven experimental data sets were considered, selection being based on the quality of the primary information contained in the temperature records (low noise, etc.).

Calculations of specific heat and hemispherical total emittance, both being rather sensitive to noise in temperature signals, particularly in the derivatives of temperature vs. time functions, required novel data reduction techniques, which are fully described in Ref. 5. Typical thermocouple and pyrometer temperature responses are shown in Fig. 1, and their first derivative vs. time functions are shown in Fig. 2. The gap in the thermocouple temperature response data were the consequence of interference due to switching of the current circuit. The optical pyrometer response was limited

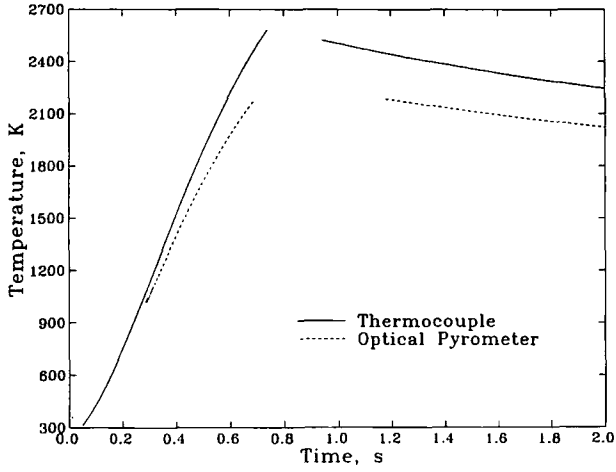

Fig. 1. Temperature transients in a pulse heating experiment.

with the saturation at 2200 K. Computation of temperature first-time derivatives involved application of recursive digital differentiation filter combined with low-pass filtering for elimination of high-frequency noise. For final specific heat, electrical resistivity, and emittance computations, these techniques were combined with multiple experiments averaging and spline-fit approximation techniques.

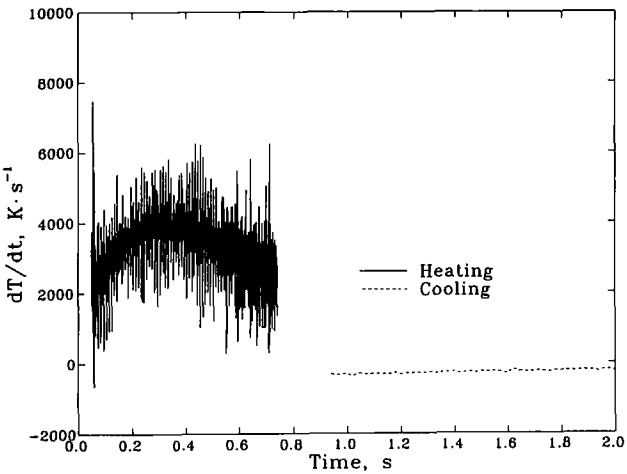

Fig. 2. Temperature–time derivative as a function of time.

3.1. Specific Heat

For specific heat calculations, seven individual data sets covering intervals between 300 and 2500 K were averaged by a cubic spline fit, resulting in an interpolated specific heat function,

$$c_p = 1.30107 \times 10^2 + 2.19036 \times 10^{-2} T - 1.91517 \times 10^{-6} T^2 + 1.27241 \times 10^{-9} T^3 \quad (6)$$

which is presented in Fig. 3. as the deviation plot in comparision with literature data. All the individual data sets were contained within a bandwidth of $\pm 2.5\%$ at its widest, the biggest difference being at both the lowest and the highest temperatures. Between 1000 and 2000 K, the margins were reduced to less than $\pm 1\%$. The maximum uncertainty in the specific heat measurements by this method using thermocouples as thermometers, given in an earlier publication [4], was estimated to be $\pm 3\%$.

Figure 3 also shows experimental results of Kirillin et al. [6] and the recommended GSSSD data [7] covering the widest temperature range, the medium-temperature results of Kraftmakher [8], medium- and high-temperature data obtained by Taylor [9], and high-temperature data reported by Cezairliyan [10], whose lowest-temperature portion lies in the upper range covered by this investigation. Results of Righini et al. [11], using the pulse heating method employing high-speed pyrometry, cover the range

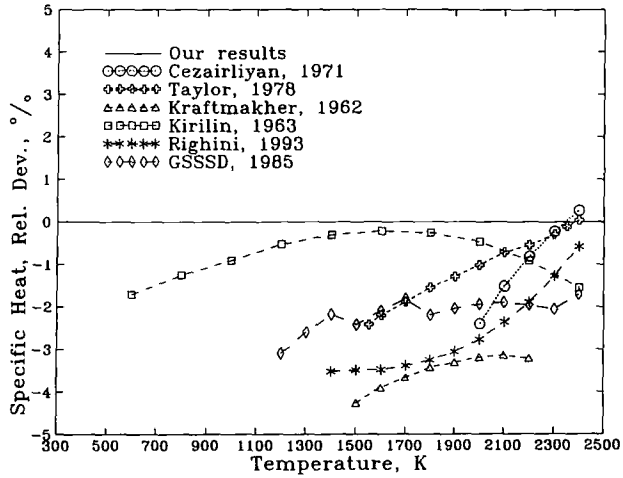

Fig. 3. Relative deviation of the specific heat of the tungsten electrode.

above 1400 K. In the range 900 to 2300 K, our results show a good agreement with the results of Kirillin et al. [6], who used drop calorimetry. Above 2000 K, our results come close to both the high-temperature pulse data of Cezairliyan [10] and the multiproperty data of Taylor [9], both sets agreeing with the function of Righini et al. [11] at about 2400 K.

3.2. Electrical Resistivity

Electrical resistivity was measured in the same experiments in which specific heat was determined. The maximum uncertainty in the electrical resistivity measurements by this method using thermocouples as thermometers is given in an earlier publication [4] and was estimated to be $\pm 1\%$. Average deviation of the measurements from the smoothed curve obtained by a spline-fit averaging was $\pm 0.1\%$.

The final electrical resistivity function (not corrected for thermal expansion), representing five data sets, in the range 300–2500 K is

$$\rho = -1.86394 \times 10^{-2} + 2.34648 \times 10^{-4} T + 4.47240 \times 10^{-8} T^2 - 5.15979 \times 10^{-12} T^3 \quad (7)$$

Electrical resistivity results compared with NBS data [12] are shown in Fig. 4; deviations of the individual experiments results from the smooth curve are in the range $\pm 2.2\%$ in the low-temperature range and $\pm 0.4\%$

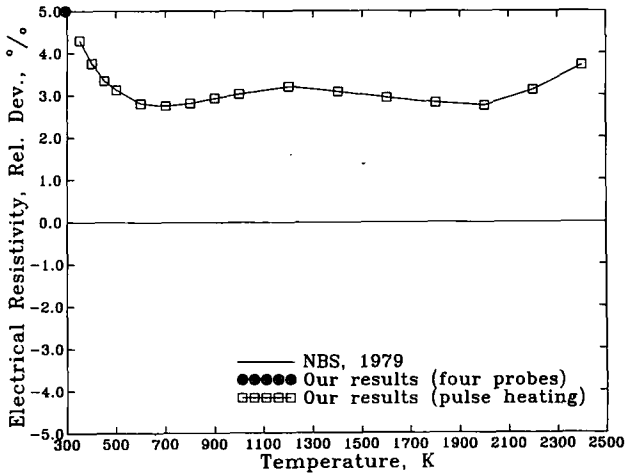

Fig. 4. Relative deviation of the electrical resistivity of the tungsten electrode.

in the high-temperature range. Figure 4 also contains a room-temperature value (293 K) measured separately after the final pulse experiment, using the four-probe technique. Somewhat larger scatter in the electrical resistivity data sets obtained idiom the individual experiments might have possibly been due to the fact that the Specimen was not heat treated prior to the pulse experiments.

3.3. Emittance Measurements

Experimental data obtained during each experiment enabled determination of both hemispherical total and normal spectral emittances. Hemispherical total emittance was obtained from Eq. (4). The interpolated average function is shown in Fig. 5 and is given by

$$\varepsilon_{ht} = -1.36903 \times 10^{-1} + 2.87003 \times 10^{-4} T - 3.75153 \times 10^{-8} T^2 \qquad (8)$$

Hemispherical total emittance values were obtained in the temperature range 1500 to 2400 K. Maximum deviations from the average values computed from several experimental data sets did not exceed $\pm 4\%$.

From simultaneous recordings of thermocouple and optical pyrometer outputs, the normal spectral emittance (at pyrometer wavelength $\lambda = 0.9\,\mu$m) was computed using Eq. (5), in the temperature interval from 1100 to 2200 K, where the ranges of these two temperature detectors overlapped.

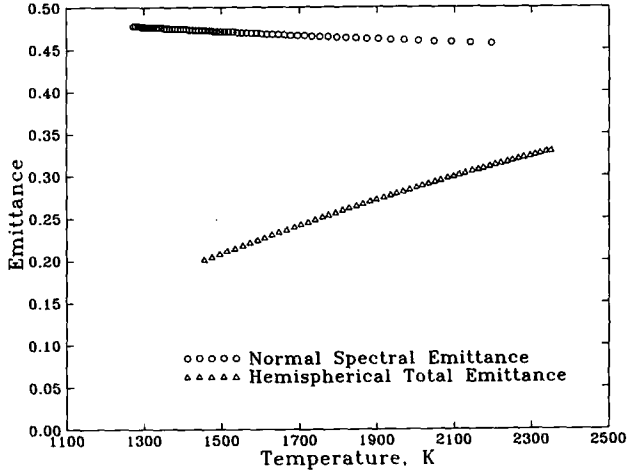

Fig. 5. Hemispherical total emittance and normal spectral emittance of the tungsten electrode.

Results of normal spectral emittance were obtained from several experimental data sets collected both during heating and cooling periods. Data shown in Fig. 5 are represented by

$$\varepsilon_{ns} = 5.28733 \times 10^{-1} - 5.01115 \times 10^{-5} T + 7.8711 \times 10^{-9} T^2 \qquad (9)$$

The maximum deviation of the individual emittance values from the above function did not exceed $\pm 2.5\%$.

ACKNOWLEDGMENT

This research was funded by the Serbian Ministry for Science and Technology. The support is gratefully acknowledged.

REFERENCES

1. A. Cezairliyan, M. S. Morse, H. A. Berman, and C. W. Beckett, *J. Res. Natl. Bur. Stand. (US)* **74**:65 (1970).
2. F. Righini, A. Rosso, and G. Ruffino, *High Temp. High Press.* **4**:597 (1972).
3. G. Pottlacher, H. Jäger, and T. Neger, *High Temp. High Press.* **19**:19 (1987).
4. A. S. Dobrosavljević and K. D. Maglić, *High Temp High Press.* **21**:411 (1989).
5. G. S. Vuković, N. Lj. Perović, K. D. Maglić, paper presented at Fourth Workshop on Subsecond Thermophysics, June 27–29, 1995, Köln, Germany.
6. V. A. Kirillin, A. E. Sheindlin, V. Ya. Chekhovskoi, and V. A. Petrov, *Zh. Fiz. Khim.* **37**:2249 (1963).
7. E. N. Fomichev, A. D. Krivorotenko, I. V. Seminko, V. J. Chehovskoi, V. D. Tarasov, and H. Irgashov, *Tabl. Stan. Spr. Dan. GSSSD* **79**:84, Moskva (1985).
8. Ya. A. Kraftmakher, *Zh. Prikl. Mekhan. I Tekhn. Fiz.* **5**:176 (1962).
9. R. E. Taylor, *J. Heat Transfer* **100**:330 (1978).
10. A. Cezairliyan, *J. Res. Natl. Bur. Stand. (US)* **75A**:283 (1971).
11. F. Righini, J. Spišiak, G. C. Bussolino, and A. Rosso, *High Temp. High Press.* **25**:193 (1993).
12. J. G. Hust and P. J. Giarratano, *Natl. Bur. Stand. (US) Spec. Publ.* **260**(52):1 (1975).